Evidence for a spin singlet state in the intermetallic semiconductor $FeGa_3$

Z. P. Yin* and W. E. Pickett
Department of Physics, University of California–Davis, Davis, California 95616, USA
(Received 16 August 2010; published 8 October 2010)

$FeGa_3$ is unusual for an intermetallic compound in displaying a semiconducting gap, on the order of 0.5 eV. Conventional density-functional based electronic-structure calculations in the local-density approximation (LDA) give a similar gap but it is expected that Fe, a 3*d* transition metal, is likely to display an on-site Coulomb repulsion U that should be taken into account, particularly in an insulating compound with some narrow bands. We analyze first-principles LDA calculations for $FeGa_3$, and then include on-site Coulomb repulsion in a mean-field way (LDA+U method) to show that, with the moderate value U on the order of 2 eV, one obtains Fe moments in antialigned Fe_2 dimers (band theory "singlets") with a band gap that still coincides with the observed gap. Counterintuitively, increasing the value of U gradually reduces the gap and finally produces an incorrect metallic state. We suggest that more experimental study should be done to distinguish between the "Fe_2 singlet" and nonmagnetic descriptions and provide calculations of the optical properties for comparison with data.

DOI: 10.1103/PhysRevB.82.155202 PACS number(s): 71.20.Lp, 75.25.−j, 78.20.−e

I. INTRODUCTION

Stoichiometric binary intermetallic compounds A_nB_m form a very large class of materials with unusual and useful properties including structural, thermal, electronic, magnetic, superconducting, and exotic correlated behavior. Structurally, many of these have high symmetry without distinctive structural characteristics. There has been effort[1–3] to categorize their preferred crystal structures into disjoint classes based on atomic properties but these are necessarily confined to crystal classes that have several members.

It is uncommon for a binary intermetallic with small integers n,m to display unusual structural characteristics such as clustering, especially when the individual atoms rarely show such behavior. The compound $FeGa_3$ is distinctive, though not unique, in this regard. In its tetragonal crystal structure the Fe atoms occur in pairs (dimers) oriented along the $\hat{x}$ and $\hat{y}$ directions in alternating planes perpendicular to the $\hat{z}$ axis while the Ga atoms are variously placed, considering that they have to accommodate the Fe dimers, and there are only three times as many of them. The structure, described in the following section, can be contrasted with the isovalent compound $FeAl_3$. $FeAl_3$ was reported in a $C2/m$ space group,[4] with 100 atoms per cell ($Z=25$). In this complex cell there are an assortment of Fe-Al and Al-Al distances. The five distinct Fe sites are (9–12)-fold coordinated, with two sites having Fe-Fe distances on the order[5] of 3 Å. There is no clear relation to the $FeGa_3$ structure, discussed below. Evidently there is some specific driving force, not yet identified, that produces the distinctive Fe_2 dimer feature in $FeGa_3$.

It is of course the physical properties and not simply the structure, of $FeGa_3$ that makes it of current interest. This intermetallic compound, reasonably close packed, has been found to be insulating, with a gap in the vicinity of 0.5 eV, as inferred from magnetic susceptibility (0.29–0.45 eV) and from photoemission experiments (less than 0.8 eV).[6] Hadano *et al.*[7] inferred gap values of 0.47–0.54 eV from electrical resistivity and Hall coefficient above 300 K.

The material is diamagnetic with susceptibility $\chi\sim 4\times 10^{-5}$ emu/mole Fe, weakly temperature dependent, below 400 K, with some upturn below 50 K. ^{57}Fe Mössbauer spectra showed no evidence of magnetic order, and it was concluded[6] that the behavior is consistent with nonmagnetic (NM) Fe in this compound. Studies of the transport behavior by Hadano *et al.*[7] revealed indication of small doping in their samples, and an impressively large thermopower reaching -350 μV/K around room temperature. The T-linear heat capacity is consistent with a weakly doped semiconductor. Thus existing data is consistent with stoichiometric $FeGa_3$ being a simple, nonmagnetic semiconductor.

The electronic structure of $FeGa_3$ (and isovalent $RuGa_3$ and $OsGa_3$) has been presented by Häussermann *et al.*[8] and by Imai and Watanabe,[9] obtaining within the standard local-density approximation (LDA) a semiconductor with a gap near 0.5 eV, consistent with experiments, and we confirm this result (described below). However, the presence of Fe atoms poses the question of possible magnetic behavior of Fe in this compound, and the structure with its unusual Fe dimers also suggests more investigation may be worthwhile. Our studies have been motivated by the question: will intra-atomic repulsion (Hubbard U) of a moderate magnitude on the Fe atoms produce a magnetic moment? If so, will this destroy the semiconducting result and other agreement with experiment? We show that antialigned moments of the Fe dimers (the band theory approximation of spin singlets) provides an alternative explanation of the observed electronic structure that indicates the need for further experimental studies of $FeGa_3$ to distinguish between the alternatives.

II. CRYSTAL STRUCTURE

The intermetallic semiconductor $FeGa_3$ crystallizes in tetragonal space group $P4_2/mnm$ (#136) with $Z=4$. Its lattice constants[8] are $a=6.2628$ Å and $c=6.5546$ Å. Fe atoms occupy the 4*f* Wyckoff position (x, x, 0) ($x\sim 0.344$) with relatively high-site symmetry $m2m$ and form dimer pairs along (110) direction in $z=0$ plane and along $(1\bar{1}0)$ direction in z

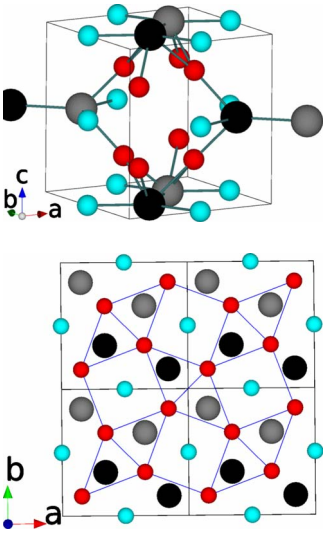

FIG. 1. (Color online) Crystal structure of $FeGa_3$ showing the tetragonal unit cell (top panel) and top view along c axis (bottom panel). Fe atoms (bigger radii) form dimer pairs along (1,1) and $(1,\bar{1})$ directions and Ga2 atoms (smaller red/black) form a 3^2434 net whose cubes are centered by Ga1 atoms (smaller light-blue/gray). The figures are plotted using the VESTA program (Ref. 10).

$=1/2$ plane (see Fig. 1). Ga2 atoms occupy the low symmetry $8j$ Wyckoff position (x',x',z) $(x'\sim 0.156, z\sim 0.262)$ with site symmetry m. They form a slightly corrugated net stacking (3^2434 in solid state chemistry terminology) on top of each other along the c direction, resulting in a tetragonal assembly of columns of rhombic prisms and slightly deformed cubes. Half of the rhombic prisms are centered by the Fe dimer pairs and the centers of the cubes are occupied by Ga1 atoms with $4c$ Wyckoff position (0,0.5,0) and site symmetry $2/m$. The distances of Fe-Fe, Fe-Ga, and Ga-Ga are shown in Table I. The 2.77 Å separation within the Fe atoms in the dimers here is 11.5% bigger than the nearest Fe-Fe distance of 2.48 Å in the bcc iron metal.

III. CALCULATIONAL METHODS

We have performed first-principles calculations on the $FeGa_3$ compound, as well as a parallel compound $RuGa_3$, in the framework of density functional theory[11,12] with local (spin) density approximation of Perdew and Wang,[13] often referred to as PW92. We have also compared with the PBE generalized gradient potential[14] exchange-correlation (XC) functional, and have looked at both with and without the Coulomb repulsion U for the d shells of the transition metals. We have used the full-potential local-orbital code[15] (FPLO7 and FPLO8) and the full-potential linearized augmented plane-wave (LAPW)+local orbitals method as implemented in WIEN2K.[16] In the LDA+U calculations, we have compared results using both the fully localized limit (FLL) and around mean field (AMF) schemes for the double counting term, with moderate values of U and a fixed Hund's $J=0.625$ eV. Unless otherwise specified, the results presented in this paper are obtained using the PW92 XC functional and FLL double counting for LDA+U calculations, in the FPLO7 program.

TABLE I. Interatomic distances (in angstrom) in $FeGa_3$. Structural parameters are from Ref. 8. Letter "n" means the number of equivalent atoms that share the same distance with the host atom. The Fe-Fe distance in bcc Fe metal is 2.4825 Å.

Atom	Atom	n	Distance
Fe	Ga1	2	2.36
	Ga2	2	2.39
	Ga2	4	2.50
	Fe	1	2.77
Ga1	Fe	2	2.36
	Ga2	4	2.83
	Ga2	4	2.92
	Ga1	2	3.28
Ga2	Fe	1	2.39
	Fe	2	2.50
	Ga2	1	2.76
	Ga1	2	2.83
	Ga1	2	2.92
	Ga2	1	3.12
	Ga2	4	3.35
	Ga2	1	3.43

IV. ELECTRONIC STRUCTURE

A. Analysis within LDA/GGA

As mentioned above, the electronic structure of $FeGa_3$ (and isovalent $RuGa_3$ and $OsGa_3$) was calculated by Häussermann *et al.* using the VASP code.[8] They obtained a band gap of about 0.3 eV, which is in the range of experimental values. Using the CASTEP planewave code with ultrasoft pseudopotentials, Imai and Watanabe[9] calculated the energy gap to be about 0.5 eV. We have obtained an energy gap of 0.4–0.54 eV using a variety of exchange-correlation potentials in the FPLO7 and WIEN2K codes. We do not make any distinction between LDA and generalized gradient approximation (GGA) results because the differences are minor.

The complicated structure with 16 atoms per cell makes analysis of the electronic structure and the cause of the gap, challenging to analyze and understand. In Fig. 2 we display the band structure of $FeGa_3$ in a region covering the Fe $3d$ band contribution, with LDA and no magnetism (NM, as in previous work). Below we compare with LDA+U results shown in the lower panel of this figure. First, we note that the Ga $4p$ character is spread rather uniformly throughout the states within a few electron volt of the gap. Distinctions between the Ga1 and Ga2 contributions to specific bands can be strong but the zone-averaged distribution is uninteresting and is not shown.

It is most important to analyze the Fe $3d$ character. We will refer both to the Fe orbitals in the crystal coordinate system $(x,y,z$, hence d_{xy}, etc.) and in a rotated local coordinate system (45° around the z axis) in which the two Fe atoms in a dimer lie along the x' axis. Below the gap lies the most distinctive feature of the bands: a set of four very flat bands (one for each Fe in the cell, or a pair for each dimer)

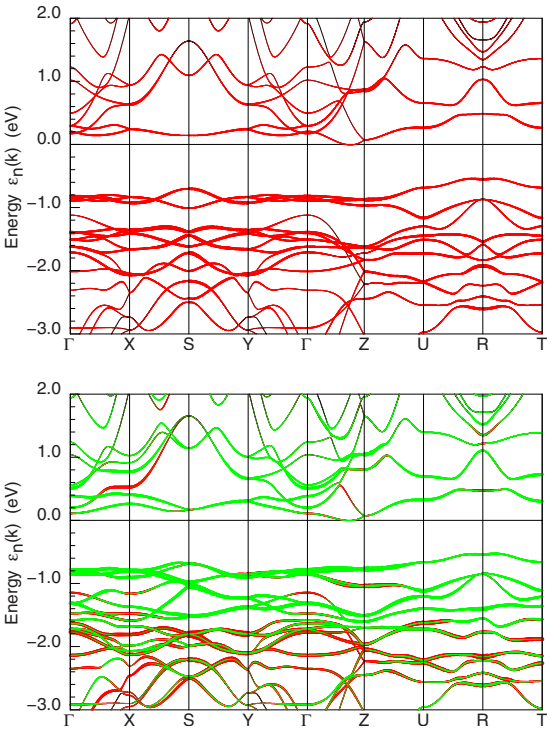

FIG. 2. (Color online) Top panel: Fe 3*d* fatbands for NM $FeGa_3$. Bottom panel: Fe 3*d* fatbands for AFM $FeGa_3$. In the AFM state, the LDA+*U* method with $U=2.0$ eV and $J=0.625$ eV is applied which results in a magnetic moment on Fe about $0.6\mu_B$.

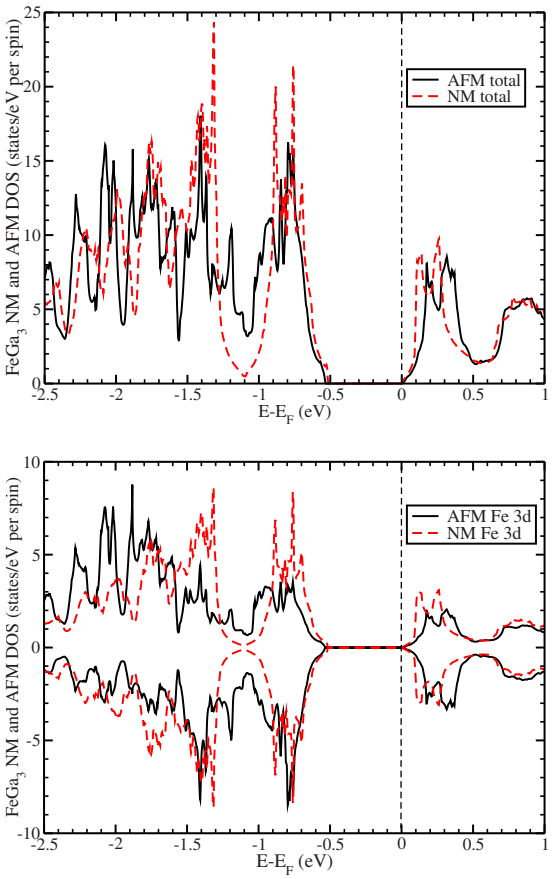

FIG. 3. (Color online) Top panel: total DOS for the AFM state, compared to that of the NM state. Note that the band gaps are equal in spite of many differences in the electronic structure (see text). Bottom Panel: spin-projected Fe 3*d* DOS of the nonmagnetic and antiferromagnetic $FeGa_3$, note particularly the filling in of the pseudogap around −1 eV in the minority DOS (plotted downward). The LDA+*U* method with $U=2.0$ eV, $J=0.625$ eV produces these results, and gives a magnetic moment on Fe of about $0.6\mu_B$.

with full width at half maximum of about 0.3 eV. These are strongly $d_{x^2-y^2}$ in character, with some mixing of d_{xz}, d_{yz} (which in the rotated system would be expected to be primarily $d_{x'z'}$ due to its $dd\pi$ overlap versus the $dd\delta$ overlap of $d_{y'z'}$ orbitals). This complex of flat bands reflects a small splitting of bonding and antibonding $d_{x^2-y^2}$ (i.e., $d_{x'y'}$) states on each of the two dimers, with little actual dispersion, reflecting localized states. The band splitting at Γ, ~0.1 eV, gives some indication of the magnitude of the bonding-antibonding splitting (coupling). Such narrow bands suggest importance of correlation effects due to intra-atomic repulsion.

The pair of bands just above the gap, which are flat in the basal plane Γ-X-M-Γ but one of which disperses to a 1 eV separation along k_z (Γ-Z) are strongly d_{z^2} in character, with admixture of d_{xy}. Most of the Fe d_{z^2} character in fact lies is a band complex 1.5 eV below the bottom of the gap, again with a rather narrow (~0.5 eV) width. The d_{xz}, d_{yz} character is more widely dispersed from −3 to 1.5 eV.

B. Analysis within LDA+*U*

The flat bands discussed above strongly suggest the importance of correlation effects due to local repulsion on Fe. We have applied a Coulomb repulsion interaction *U* (varying its strength since no good estimate is available) and a Hund's exchange $J=0.625$ eV to the Fe 3*d* electrons. A localized magnetic moment of Fe with both ferromagnetic (FM) and antiferromagnetic (AFM) orderings is obtained with any *U* value of 2 eV or larger. (The AMF functional produces similar results but requires a somewhat larger value of *U*, due to its energy penalty for magnetism.[17,18])

With all values of *U* and *J* that we tried, the total energy of the antiferromagnetically ordered state is substantially lower than that of the ferromagnetically aligned state, by more than 150 meV/Fe, so we confine our interest to AFM alignment. Considering the relative isolation of Fe dimer pairs from each other, this antialignment should be considered as the band theory counterpart of a singlet state.

With $U=2$ eV, a plausible value for Fe in an intermetallic compound, AFM ordered $FeGa_3$ has the same energy gap of 0.52 eV as in the NM state as shown in Fig. 3, with a magnetic moment on Fe of $0.6\mu_B$. In the DOS of the NM state, there is a pseudogap in the valence bands between −1.3 and −0.9 eV, between the flat four-band complex discussed above, and the remaining, more strongly bound, Fe states (see Fig. 3 and the top panel of Fig. 2). This pseudogap is narrowed and its depth is reduced significantly in the AFM state. The Fe 3*d* minority DOS of the AFM state shows a general increase at lower energy and decrease near the gap, and the change for the minority is in the opposite direction.

TABLE II. The magnetic moment m (μ_B) of Fe in the FM and AFM ordered $FeGa_3$, the energy gap Δ_g (electron volt) of AFM ordered $FeGa_3$, the total energy ΔE (meV/Fe) of AFM state compared to FM state of $FeGa_3$ (compared at the same U and J), and the effective J^* (millielectron volt) in the LDA+U calculations. J=0.625 eV are used in all the calculations. The FM and AFM states are converged to NM state when $U \leq 1.5$ eV.

U (eV)	m_{FM}	m_{AFM}	Δ_g	ΔE	$J_{Fe}S^2$
1.5	0	0	0.52	0	
2.0	0	0.62	0.52	−2.5	
2.5	1.16	1.34	0.39	−154	154
3.0	1.46	1.89	0.13	−168	168
3.5	2.58	2.34	0	−186	186
4.0	2.80	2.71	0	−152	152

Although the DOS above the gap in Fig. 3 seems little changed by the magnetism, the increase (decrease) in majority (respectively, minority) occupation upon becoming magnetic must involve a shift of spectral weight across the gap.

With increase in U, the center of the majority Fe d states moves somewhat to lower energy and the Fe magnetic moment increases. The band structures and Fe 3d characters (fatbands) of the NM and AFM states, shown in Fig. 2, have many similarities. The Fe $3d_{z^2}$ character at about −1.3 eV around the M point in the NM state moves up somewhat to −1.1 eV whereas the Fe $3d_{xz}$ and $3d_{yz}$ characters at about −1.6 eV around M point also in the NM state were pulled apart to −1.8 eV and −1.5 eV.

The sensitivity of the moment, band gap, and FM-AFM energy difference to the Coulomb interaction parameter U is presented in Table IVB. The magnetic moment of Fe in the AFM state changes rapidly as U increases through 2 eV, with the gap hardly changing initially as the moment grows, and then *decreases and vanishes* somewhere above U=3 eV. No energy gap is observed in the FM state no matter what U value is used. With the same U and J, the magnetic moments in the AFM and FM state are very similar. The total energy of the AFM state is about 160 meV/Fe lower than the FM state when U varies from 2 to 4 eV, resulting a large singlet-triplet splitting $2J_{Fe}S^2 \sim 0.32$ eV ~ 3600 K. With this large coupling J_{Fe} (we suppose that formally, S=1), the Fe singlet state formed by the Fe dimer could remain coupled beyond the melting temperature of $FeGa_3$ (Table II).

C. Observations about $RuGa_3$

Similar calculations have been applied to a parallel compound $RuGa_3$ but a magnetic solution cannot be obtained with any reasonable U value for the 4d shell of Ru within LDA+U. The bandgap for the nonmagnetic state of $RuGa_3$, shown in Fig. 4, is around 0.5 eV for the various XC potential choices. which is somewhat larger with experimental value of 0.32 eV.[19] The Ru 4d bandwidth is substantially larger than Fe 3d in the NM state as shown in Fig. 4, which indicates the Ru 4d electrons are more itinerant and therefore less correlated than Fe 3d electrons. This difference provides a natural explanation why no magnetic state is found for $RuGa_3$.

V. OPTICAL PROPERTIES

Since the band gap and general electronic structure are surprisingly similar for the AFM and NM states, we have evaluated the optical spectrum in the expectation that it can be useful in distinguishing between them. Optical spectra contain information about both occupied and unoccupied states, and the character of bands is reflected through the matrix elements, so some distinction should arise. The optical properties of the NM and AFM states of $FeGa_3$ were calculated using the WIEN2K code with the PBE functional.

The real $\varepsilon_1(\omega)$ and imaginary $\varepsilon_2(\omega)$ parts of the dielectric function for both NM and AFM states of $FeGa_3$ are presented in Fig. 5. The overriding observation, whether from the dielectric function, or from the reflectivity and optical conductivity shown in Fig. 6, or the energy loss function (not shown), is that the differences between the NM and AFM results are not very striking. Likewise, the anisotropy, as obtained from the differences between xx and zz elements of the dielectric tensor, is not large. (Recall that the Fe_2 dimers lie in the x-y plane.)

The onsets (optical bandgap) in $\varepsilon_2(\omega)$ are similar in all states and polarizations, around 0.75 eV. The differences in $\varepsilon_1(\omega)$ lie primarily in the 2.5–3.5 eV region, where NM zz is up to a factor of two larger than the others, and that the zz

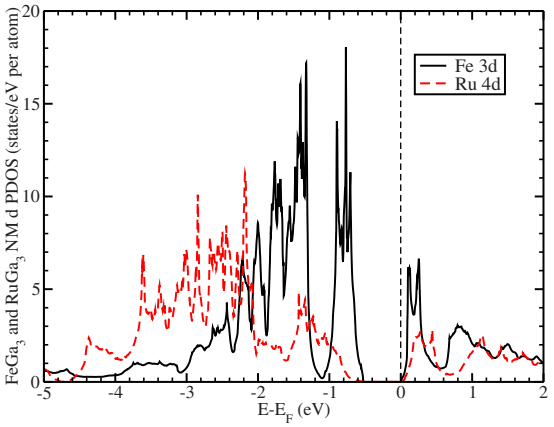

FIG. 4. (Color online) Fe 3d and Ru 4d PDOS in the NM state of $FeGa_3$ and $RuGa_3$.

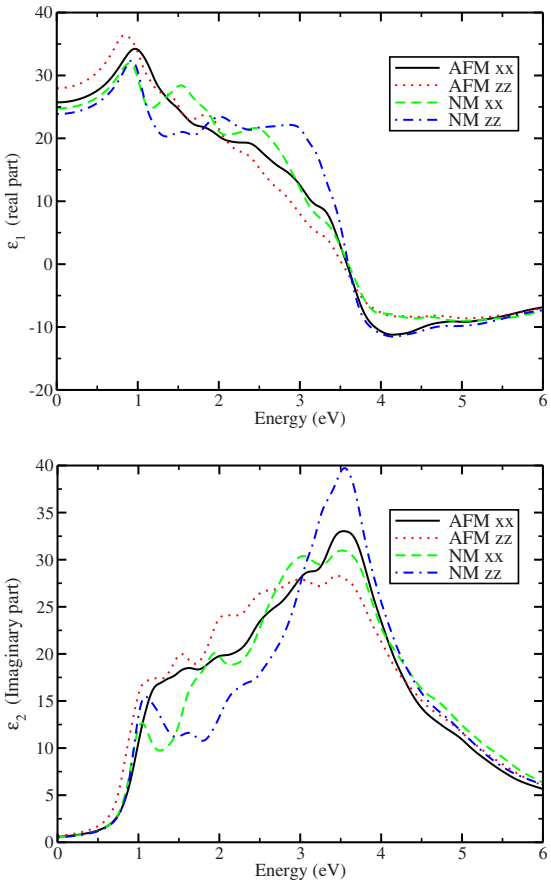

FIG. 5. (Color online) Real (top panel) and imaginary (bottom panel) part of dielectric function $\varepsilon(\omega)$ for NM and AFM states of $FeGa_3$.

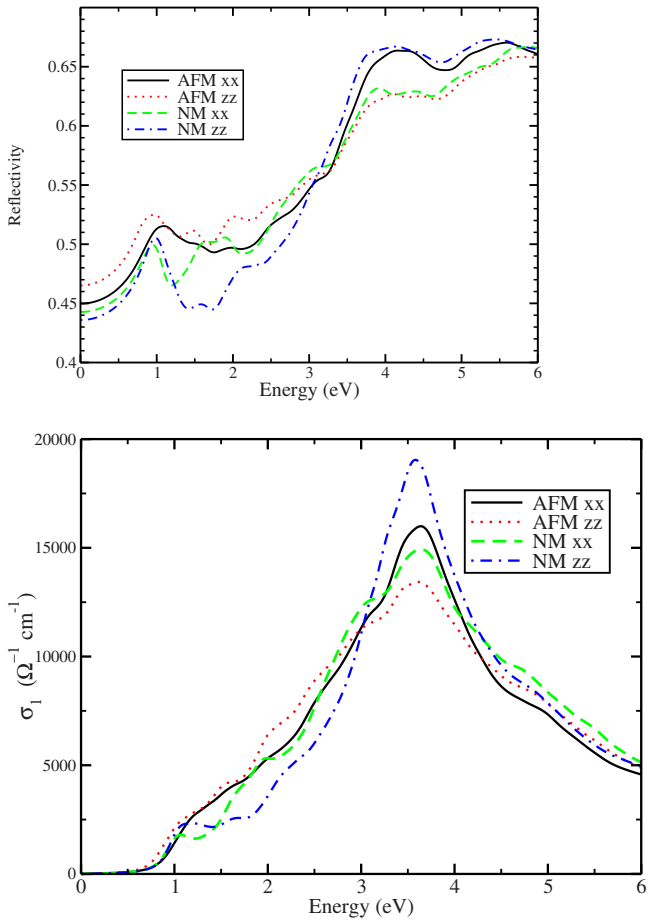

FIG. 6. (Color online) Reflectivity $R(\omega)$ and the optical conductivity, $\sigma_1(\omega)$, of the NM and AFM states of $FeGa_3$.

component of both phases shows an edge, i.e., a rapid drop at 3.5–3.7 eV. This edge is associated (via the Kramers-Kronig transform) to the more distinctive peak in $\varepsilon_2(\omega)$ in the 3.3–4 eV range. Note that these are anisotropy differences, and are similar in the NM and AFM phases and therefore of little help in distinguishing these two phases. However, due to the pseudogap structure in the NM DOS in the −1.3 to −0.9 eV range, there are substantial pseudogap structure in both the *xx* and *zz* component of both $\varepsilon_1(\omega)$ and $\varepsilon_2(\omega)$ in the 1.0–2.2 eV region in the NM state. Note there is no such pseudogap structure in the AFM state. Therefore, the NM and AFM states might be distinguishable by these pseudogap structures between 1.0 and 2.2 eV of the dielectric function.

Because the reflectivity and optical conductivity provide the most direct comparison with experiment, we provide them in Fig. 6. The reflectivities at zero frequency are all 0.45 ± 0.02 and the overall curvature are quite similar. At high energy (3.5–5.5 eV), the *xx* reflectivity is substantially larger than the *zz* component in the AFM state while it is the other way around in the NM state (i.e., the *xx* component is smaller than the *zz* component). Yet a bigger difference in the reflectivity between the NM and AFM states occurs in the 1.0–2.2 eV region again in the form of pseudogap structure in both the *xx* and *zz* components but only in the NM state. This difference also provides a chance to distinguish the two states.

In the optical conductivity $\sigma_1(\omega)$ curves, the main difference is in the height of the peak in the 3.3–4 eV region [related to the similar difference in $\varepsilon_2(\omega)$], where the spectra of the NM phase are ~15% larger for the NM phase than for AFM. Without both to compare (which will not be available experimentally), a closer comparison between the calculated curves and the data may be necessary to establish any (dis-)agreement. Possible distinction of the two states might be established by a close look at the optical conductivity in the 1.0–2.0 eV region. In the NM states, the *xx* and *zz* components of $\sigma_1(\omega)$ is relatively flat in the 1.0 eV–1.5 eV region and 1.0 eV–2.0 eV region, respectively. However, there is no flat region of the *xx* and *zz* optical conductivity in the 1.0–2.0 eV in the AFM state.

VI. SUMMARY

We have analyzed first-principles LDA calculations to the intermetallic compound $FeGa_3$, finding similar results to those in the literature when possible magnetism is neglected but noting very narrow Fe 3*d* bands just below (and above) the 0.5 eV gap. Since Fe is magnetic in many compounds even when the bands are not so flat, we have included strong interaction effects using the LDA+*U* method to check for possible magnetic phases. With a realistic value of on-site

repulsion energy $U=2$ eV ($J=0.625$ eV) the Fe atoms $FeGa_3$ become magnetic (moment of $0.6\mu_B$), and strongly prefer to be antiferromagnetically coupled, thus forming the band theory equivalents of spin singlets. Unexpectedly, the band gap remains at 0.5 eV, and decreases for larger values of U as the moment triples in size. On the contrary, with any reasonable U value in the LDA+U calculations, the Ru atoms in $RuGa_3$ (an isostructural, isovalent sister compound of $FeGa_3$) do not become magnetic. We have discussed the difference in the electronic structures of the NM and AFM states, and have presented the optical spectra in the hope that further experiments will provide a check on this possible spin-singlet state in an intermetallic compound.

ACKNOWLEDGMENT

This work was supported by DOE under Grant No. DE-FG02-04ER46111.

*Present address: Department of Physics and Astronomy, Rutgers University, Piscataway, NJ 08854, USA.

[1] P. Villars, J. Less-Common Met. **92**, 215 (1983).
[2] D. G. Pettifor, J. Phys. C **19**, 285 (1986).
[3] Y. Harada, M. Morinaga, J.-I. Saito, and Y. Takagi, J. Phys.: Condens. Matter **9**, 8011 (1997).
[4] P. J. Black, Acta Crystallogr. **8**, 43 (1955).
[5] P. J. Black, Acta Crystallogr. **8**, 175 (1955).
[6] N. Tsujii, H. Yamaoka, M. Matsunami, R. Eguchi, Y. Ishida, Y. Senba, H. Ohashi, S. Shin, T. Furubayshi, H. Abe, and H. Kitazawa, J. Phys. Soc. Jpn. **77**, 024705 (2008).
[7] Y. Hadano, S. Narazu, M. A. Avila, T. Onimaru, and T. Takabatake, J. Phys. Soc. Jpn. **78**, 013702 (2009).
[8] U. Häussermann, M. Boström, P. Viklund, Ö. Rapp, and T. Björnängen, J. Solid State Chem. **165**, 94 (2002).
[9] Y. Imai and A. Watanabe, Intermetallics **14**, 722 (2006).
[10] K. Momma and F. Izumi, J. Appl. Crystallogr. **41**, 653 (2008).
[11] P. Hohenberg and W. Kohn, Phys. Rev. **136**, B864 (1964).
[12] W. Kohn and L. J. Sham, Phys. Rev. **140**, A1133 (1965).
[13] J. P. Perdew and Y. Wang, Phys. Rev. B **45**, 13244 (1992).
[14] J. P. Perdew, K. Burke, and M. Ernzerhof, Phys. Rev. Lett. **77**, 3865 (1996).
[15] K. Koepernik and H. Eschrig, Phys. Rev. B **59**, 1743 (1999).
[16] P. Blaha, K. Schwarz, G. K. H. Madsen, D. Kvasnicka, and J. Luitz, in *WIEN2K*, edited by K. Schwarz (Technische Universität Wien, Austria, 2001).
[17] I. I. Mazin, M. D. Johannes, L. Boeri, K. Koepernik, and D. J. Singh, Phys. Rev. B **78**, 085104 (2008).
[18] E. R. Ylvisaker, W. E. Pickett, and K. Koepernik, Phys. Rev. B **79**, 035103 (2009).
[19] Y. Amagai, A. Yamamoto, T. Iida, and Y. Takanashi, J. Appl. Phys. **96**, 5644 (2004).